

Phosphorus(V) Porphyrin–Azoarene Conjugates: Synthesis, Spectroscopy, cis–trans Isomerization, and Photoswitching Function

D. Raghunath Reddy and Bhaskar G. Maiya*

School of Chemistry, University of Hyderabad, Hyderabad 500 046, India

Received: September 14, 2002; In Final Form: February 10, 2003

A series of photochemically active, “axial-bonding” type phosphorus(V) porphyrin–azoarene (P–A) conjugates, viz., [(TTP)P^V(-O-AZM)₂]⁺, [(TTP)P^V(-O-AZT)₂]⁺, [(TTP)P^V(-O-AZB)₂]⁺, and [(TTP)P^V(-O-AZN)₂]⁺ (TTP is 5,10,15,20-tetra(4-methylphenyl)porphyrinato dianion and O-AZM, O-AZT, O-AZB, and O-AZN are the axially coordinated 4-methoxy azophenoxo, 4-methyl azophenoxo, azophenoxo, and 4-nitro azophenoxo ligands, respectively) have been synthesized and fully characterized by mass (FAB), infrared, UV–visible, proton nuclear magnetic resonance (1D and ¹H-¹H COSY), and electrochemical methods. The spectroscopic data suggest that the two azoarene subunits in these hexa-coordinated systems exist in their trans isomeric forms and that there is minimal ground-state interaction between the axial ligands and the basal porphyrin π plane in each case. Continuous irradiation of CH₃CN solutions containing these new P–A conjugates at 345±5 nm results in isomerization of the phosphorus-bound azoarene subunits to produce the respective cis forms, as revealed by the UV–visible spectral data. The reverse, thermal back reactions have also been spectrally monitored, and the trans forms could be recovered quantitatively. Rate measurements and detailed analysis of the kinetic data have been made for both the forward and the reverse reactions. Fluorescence due to the porphyrin components of the “trans forms” of [(TTP)P^V(-O-AZM)₂]⁺, [(TTP)P^V(-O-AZT)₂]⁺, and [(TTP)P^V(-O-AZB)₂]⁺ are quenched in comparison with that due to a porphyrin reference compound [(TTP)P^V(OH)₂]⁺. Moreover, fluorescence intensities of the respective “cis forms” are less than the corresponding “trans forms” in each case. The photochemical/thermal trans ↔ cis isomerization reactions of the axial azoarene subunits and the consequent modulation of the fluorescence intensities have been repeated several times with minimal loss of the material. Based on the results of detailed photochemical studies carried out with these new P–A conjugates, it is argued that distance dependence of the photoinduced electron transfer occurring between the axial azoarene subunit and the singlet porphyrin is responsible for their effective and stable photoswitching function.

Introduction

Photoreversible compounds, where the process of reversibility is based on photochemically induced interconversions, are particularly attractive materials for fabricating molecule-based switching devices.^{1–5} Molecular/supramolecular systems that incorporate an azobenzene chromophore in their architecture are an important class of such photochromic materials owing to the facile and reversible cis–trans isomerization reactions of this photoactive chromophore. Although UV–visible spectroscopy has long been the most commonly used detection technique for sensing the activities of such materials, the necessity of having other means of detection (viz., complexation of ions, refractive index, electrochemical behavior, luminescence, etc.) is increasingly being realized in recent years. A number of molecular assemblies, which can potentially exhibit modulation of their fluorescence/redox properties that is induced by cis–trans isomerization of the appended azobenzene subunit/s are being developed by many researchers.^{6–12} Among such systems, those based on porphyrins and their derivatives are of relevance to the present work. Porphyrin-based systems are useful in the design of devices involving long-wavelength excitation because of the favorable spectral and luminescence properties of these extensively π -conjugated macrocyclic sys-

tems. However, barring a recent exception,¹³ many earlier attempts to build functionally active, porphyrin-based photoswitches with the switching action being effected by the azobenzene moiety have been curiously unsuccessful.^{14–18} Extending on our recent successful demonstration of the photoswitching function by a prototype phosphorus(V) (P(V)) porphyrin–azobenzene system,¹⁹ we describe here the design, synthesis, spectral characterization, and cis–trans isomerization induced luminescence on/off function of a series of hexa-coordinated P(V)porphyrin–azoarene (P–A) conjugates, Figure 1. This study illustrates the potential utility of this class of “axial-bonding” type P(V) porphyrins as photoswitching devices.

Experimental Section

Materials. The chemicals and solvents utilized in this study were purchased from either Aldrich Chemical Co. (U.S.A.) or B. D. H. (Mumbai, India). The solvents utilized for spectroscopic and electrochemical experiments were further purified using the standard procedures.²⁰

Synthesis. The precursor porphyrins, 5,10,15,20-tetra(4-methylphenyl)porphyrin (**H₂TTP**),²¹ and its P(V) derivatives 5,10,15,20-tetra(4-methylphenyl)porphyrinato phosphorus(V) dichloride [(TTP)P^V(Cl)₂]⁺ and 5,10,15,20-tetra(4-methylphenyl)porphyrinato phosphorus(V) dihydroxide [(TTP)P^V(OH)₂]⁺,²² have been synthesized by employing the reported

* To whom correspondence should be addressed.

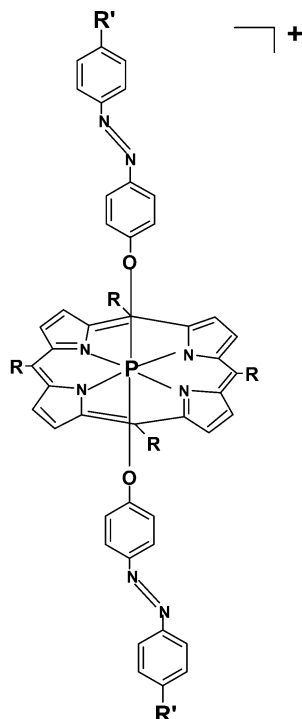


Figure 1. Structures of the P–A conjugates investigated in this study (R = 4-methylphenyl group).

methods. 5,10,15,20-Tetraphenylporphyrin (H_2TTP) and 5,10,15,20-tetraphenylporphyrinato zinc(II) ($[(\text{TTP})\text{Zn}^{\text{II}}]$), the reference compounds used during the fluorescence studies, were also synthesized by the literature procedures.²¹ Non-porphyrinic precursors 4-hydroxy-4'-methoxyazobenzene ($\text{AZM}(\text{OH})$), 4-hydroxy-4'-methylazobenzene ($\text{AZT}(\text{OH})$), 4-hydroxyazobenzene ($\text{AZB}(\text{OH})$), and 4-hydroxy-4'-nitroazobenzene ($\text{AZN}(\text{OH})$) were prepared by adapting the standard procedure.²³ P–A conjugates, $[(\text{TTP})\text{P}^{\text{V}}(-\text{O}-\text{AZM})_2]^+$, $[(\text{TTP})\text{P}^{\text{V}}(-\text{O}-\text{AZT})_2]^+$, $[(\text{TTP})\text{P}^{\text{V}}(-\text{O}-\text{AZB})_2]^+$, and $[(\text{TTP})\text{P}^{\text{V}}(-\text{O}-\text{AZN})_2]^+$, have been synthesized starting from $[(\text{TTP})\text{P}^{\text{V}}(\text{Cl})_2]^+$ and the above hydroxy azoarene precursors, as detailed below.

Preparation of the P–A Conjugates. $[(\text{TTP})\text{P}^{\text{V}}(\text{Cl})_2]^+$ (0.10 g, 0.013 mmol) and ~ 2 mmol of either $\text{AZM}(\text{OH})$ (0.46 g), $\text{AZT}(\text{OH})$ (0.42 g), $\text{AZB}(\text{OH})$ (0.40 g), or $\text{AZN}(\text{OH})$ (0.49 g) were dissolved in pyridine (20 mL) and refluxed for 2 h under the nitrogen atmosphere. The solvent was removed under reduced pressure, and the crude product was chromatographed on silica gel (60–200 mesh size). Elution with CHCl_3 removed a faint red fraction which was discarded in each case. Changing the eluent to CHCl_3 – CH_3OH (10:1 v/v) mixture removed the desired product as a purple-brown band. The solvent was evaporated under reduced pressure, and the resulting solid was recrystallized from CH_2Cl_2 –hexane to give pure solid product. Yields varied typically between 70 and 80%.

IR (KBr Pellet) and FAB-MS (M/z) Data. $[(\text{TTP})\text{P}^{\text{V}}(-\text{O}-\text{AZM})_2]^+$: IR: 887 cm^{-1} ($\nu_{\text{P}-\text{O}}$), 1489 cm^{-1} ($\nu_{\text{N}=\text{N}}$); FAB-MS:

$[\text{M}]^+$ 1153, $[\text{M}-(\text{C}_{13}\text{H}_{11}\text{N}_2\text{O}_2)]^+$ 926, $[\text{M}-2(\text{C}_{13}\text{H}_{11}\text{N}_2\text{O}_2)]^+$ 699 (base peak). $[(\text{TTP})\text{P}^{\text{V}}(-\text{O}-\text{AZT})_2]^+$: IR: 885 cm^{-1} ($\nu_{\text{P}-\text{O}}$), 1489 cm^{-1} ($\nu_{\text{N}=\text{N}}$); FAB-MS: $[\text{M}]^+$ 1121, $[\text{M}-(\text{C}_{13}\text{H}_{11}\text{N}_2\text{O})]^+$ 910, $[\text{M}-2(\text{C}_{13}\text{H}_{11}\text{N}_2\text{O})]^+$ 699 (base peak). $[(\text{TTP})\text{P}^{\text{V}}(-\text{O}-\text{AZB})_2]^+$: IR: 883 cm^{-1} ($\nu_{\text{P}-\text{O}}$), 1489 cm^{-1} ($\nu_{\text{N}=\text{N}}$); FAB-MS: $[\text{M}]^+$ 1093, $[\text{M}-(\text{C}_{12}\text{H}_9\text{N}_2\text{O})]^+$ 896, $[\text{M}-2(\text{C}_{12}\text{H}_9\text{N}_2\text{O})]^+$ 699 (base peak). $[(\text{TTP})\text{P}^{\text{V}}(-\text{O}-\text{AZN})_2]^+$: IR: 847 cm^{-1} ($\nu_{\text{P}-\text{O}}$), 1489 cm^{-1} ($\nu_{\text{N}=\text{N}}$); FAB-MS: $[\text{M}]^+$ 1183, $[\text{M}-(\text{C}_{12}\text{H}_8\text{N}_3\text{O}_3)]^+$ 941, $[\text{M}-2(\text{C}_{12}\text{H}_8\text{N}_3\text{O}_3)]^+$ 699 (base peak).

Methods. Care was taken to avoid the entry of direct, ambient light into the samples in all the spectroscopic and electrochemical experiments described below. Unless otherwise specified, all of the experiments were carried out at 293 ± 3 K.

FAB mass spectra were recorded with a JEOL SX 102/DA-6000 mass spectrometer/data system. Infrared spectra were recorded (KBr pellets) with a Jasco model 5300 FT-IR spectrometer. UV–visible spectra were recorded with a Shimadzu model UV-3101-PC UV–visible spectrophotometer. Concentration of the samples used for these measurements ranged from $\sim 2 \times 10^{-6}$ M (porphyrin Soret bands) to $\sim 6 \times 10^{-5}$ M (porphyrin Q-/azoarene bands). The ^1H NMR spectra were recorded with a Bruker NR-200 AF–FT NMR spectrometer using CDCl_3 as the solvent and tetramethylsilane (TMS) as an internal standard. The proton decoupled ^{31}P NMR spectra were also recorded with the same instrument albeit, with an operating frequency of 80.5 MHz and with 85% H_3PO_4 as an external standard. Cyclic- and differential-pulse voltammetric experiments (CH_3CN , 0.1 M tetrabutylammonium perchlorate, TBAP) were performed on a CH Instruments model CHI 620A electrochemical analyzer as detailed in our previous studies (working and auxiliary electrodes: Pt; reference electrode: SSCE).^{24–26} Fc^+/Fc (Fc = ferrocene) couple was used to calibrate the redox potential values.

Steady-state fluorescence spectra were recorded using a Jasco model FP-777 spectrofluorimeter. The emitted quanta were detected at right angle to the incident beam. The utilized concentrations of the fluorophores were such that the optical densities (O.D.) at the excitation wavelengths were always less than 0.2. The fluorescence quantum yields (ϕ_f) were estimated by integrating the areas under the fluorescence curves and by using $[(\text{TTP})\text{Zn}^{\text{II}}]$, ($\phi_f = 0.036$ in CH_2Cl_2) as the standard.²⁷ Refractive index corrections have been incorporated while reporting the fluorescence data in various solvents.²⁸ Triplet–triplet differential absorption spectra and the triplet state lifetimes were measured using nanosecond laser flash photolysis.²⁹ For laser excitation at 532 nm (8 ns width, 30 mJ) a Quanta Ray GCR-2 Nd:YAG laser was employed in the right angle geometry and a 1 cm path length cell was used in this investigation. The signals were detected using a pulsed xenon lamp, Czerny Turner monochromator and R-928 PMT. The signals were captured in a Hewlett-Packard 54201A digital storage oscilloscope. The data were transferred to the computer and analyzed using an in-house software. The experiments were carried out by purging the solution with argon for 20 min.

Steady-state photolysis of CH_3CN solutions of the P–A conjugates and their respective azoarene precursors were carried out using a Xe-arc lamp (150 W, PTI model A1010) as the light source. The required wavelength for the irradiation (345 ± 5 nm) was isolated from the source using a PTI model S/N 1366 MONO monochromator. A 10-mm light path-length quartz cell was used for these measurements. All of the samples were degassed by purging with nitrogen gas before photoirradiation. Absorbances of the samples being irradiated were monitored as a function of time in the wavelength region 275–700 nm.

TABLE 1: NMR Data

compound	¹ H NMR data ^a δ, ppm									³¹ P NMR data ^b δ, ppm
	peripheral protons				axial ligand protons ^c					
	H _β (J _{PH})	H _α H _m (J _{HH})	CH ₃	H _o (J _{HH} , J _{PH}) [Δδ]	H _m (J _{HH}) [Δδ]	H _o ' (J _{HH}) [Δδ]	H _m ' (J _{HH}) [Δδ]	H _p /CH ₃ [Δδ]		
[(TTP) ^P (-O-AZM) ₂] ⁺	9.06 (d, 8H) (3.3)	7.66 (d, 8H) (7.9)	7.51 (d, 8H) (7.9)	2.59 (s, 12H)	2.37 (d, 4H) (8.8) [4.6]	6.50 (d, 4H) (8.8) [1.3]	7.59 (d, 4H) (9.0) [0.26]	6.87 (d, 4H) (9.0) [0.1]	3.82 (s, 6H) [0.07]	-197.2
[(TTP) ^P (-O-AZT) ₂] ⁺	9.07 (d, 8H) (3.7)	7.66 (d, 8H) (7.9)	7.51 (d, 8H) (7.9)	2.60 (s, 12H)	2.37 (d, 4H) (9.0) [4.5]	6.53 (d, 4H) (9.0) [1.3]	7.51 (d, 4H) (8.0) [0.32]	7.17 (d, 4H) (8.0) [0.1]	2.35 (s, 6H) [0.08]	-197.4
[(TTP) ^P (-O-AZB) ₂] ⁺	9.08 (d, 8H) (3.4)	7.66 (d, 8H) (7.7)	7.51 (d, 8H) (7.7)	2.59 (s, 12H)	2.40 (d, 4H) (8.0) [4.5]	6.56 (d, 4H) (8.0) [1.3]	7.58 (d, 4H) (8.0) [0.31]	7.38 (d, 4H) (8.0) [0.1]		-194.9
[(TTP) ^P (-O-AZN) ₂] ⁺	9.10 (d, 8H) (3.7)	7.67 (d, 8H) (7.4)	7.52 (d, 8H) (7.4)	2.59 (s, 12H)	2.45 (d, 8H) (8.5) [4.5]	6.64 (d, 4H) (8.5) [1.3]	7.70 (d, 4H) (8.5) [0.26]	8.23 (d, 4H) (8.5) [0.14]		-195.5

^a Spectra were measured in CDCl₃ using TMS as an internal standard. Error limits: δ, ±0.01 ppm; J, ±1 Hz. ^b Spectra were measured in CDCl₃ using 85% H₃PO₄ as an external standard. Error limits: δ, ±0.5 ppm. ^c Δδ values given within the square parentheses refer to ring current induced shifts for the resonances due to various protons on the axial azoaryloxo ligands, i.e., Δδ = δ (free azophenol) - δ (porphyrin).

Irradiation was discontinued upon attainment of the photo-stationary equilibrium (PSE; i.e., when no further change in absorbance at the 345 nm band occurred). The trans-to-cis isomerization rate constant, k_{t-c} , was evaluated from the change in absorbance with respect to time t (eq 1)

$$k_{t-c}t = \ln\{(A_0 - A_\infty)/(A_t - A_\infty)\} \quad (1)$$

where A_0 , A_t , and A_∞ denote the absorbance at $t = 0$, t and ∞ , respectively. Both k_{t-c} and A_∞ were evaluated by a nonlinear least-squares calculation. Quantum yields of the photochemical trans-to-cis isomerization (Φ_{t-c}) were determined using azobenzene as the working standard ($\Phi_{t-c} = 0.11$ in hexane).³⁰ The intensity of light was measured using ferrioxalate actinometry.³¹

Immediately upon attainment of the PSE, each sample was kept aside in the dark to monitor the thermal cis-to-trans reaction. The spectra were run in the wavelength region 275–700 nm at regular intervals of time. The cis-to-trans isomerization rate constant, k_{c-t} , was evaluated from the change in absorbance at 345 nm and using a kinetic treatment similar to that described above for the trans-to-cis isomerization reaction.

Results and Discussion

Synthesis and Characterization. Relying largely on oxophilicity of the P(V) ion and by adopting a protocol that we had developed earlier for the synthesis of various “axial-bonding” type P(V), Sn(IV), and Ge(IV) porphyrin arrays and donor-acceptor (D-A) compounds,^{32–36} synthesis of the four new P-A conjugates has been accomplished here in good-to-moderate yields. These aryloxo P(V) porphyrins are readily synthesizable and stable species as was the case with a host of aryloxo derivatives of metalloporphyrin species previously reported by us^{32–36} and others.^{22,37} Each new compound was fully characterized by FAB-MS, IR, UV-visible, and ¹H NMR (1D and ¹H-¹H COSY) methods.

The ¹H NMR spectrum of each new metalloporphyrin synthesized during this study shows characteristic, porphyrin ring-current induced upfield shifts³⁸ for the protons on the axial aromatic ligands, with the magnitude of shift for a given proton ($\Delta\delta = \delta_{\text{free azophenol}} - \delta_{\text{complexed}}$) being a function of its separation distance from the porphyrin π plane. This fact is illustrated in

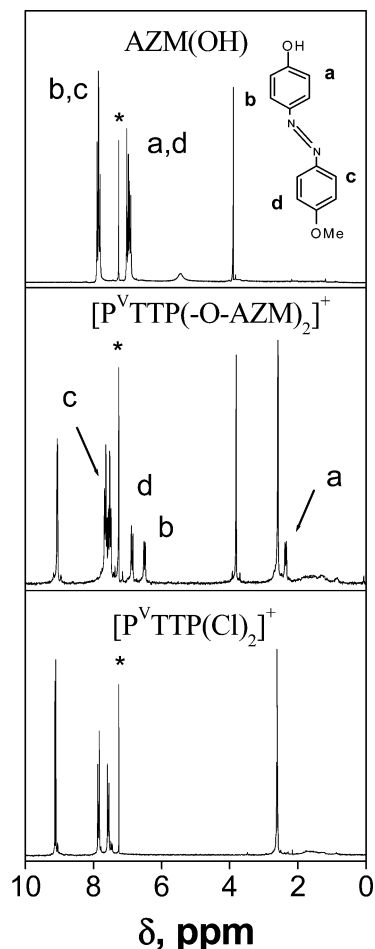


Figure 2. ¹H NMR spectra (CDCl₃, TMS) of AZM(OH), [(TTP)^P(-O-AZM)₂]⁺, and [(TTP)^P(Cl)₂]⁺.

Figure 2 which compares the spectrum of [(TTP)^P(-O-AZM)₂]⁺ with those of its unlinked, synthetic precursors, viz., [(TTP)^P(Cl)₂]⁺ and AZM(OH). As seen, protons of the type a , b , c , and d of AZM(OH) are upfield shifted upon axial coordination in [(TTP)^P(-O-AZM)₂]⁺. The situation is similar with the other P-A conjugates investigated here, as revealed by the corresponding $\Delta\delta$ values summarized in Table 1. On

TABLE 2: Redox Potential Data (CH₃CN, 0.1 M TBAP)^a

compound	reduction $E_{1/2}$, V (vs SCE)	$\Delta E_{1/2}$ ^b	oxidation ^c $E_{1/2}$, V (vs SCE)	E_{CT} , ^d eV
[(TTP)P ^V (OH) ₂] ⁺	-0.61, -0.96,			
[(TTP)P ^V (-O-AZM) ₂] ⁺	-0.37, -0.79	0.42	+ 1.30	1.67
[(TTP)P ^V (-O-AZT) ₂] ⁺	-0.43, -0.86	0.43	+ 1.49	1.92
[(TTP)P ^V (-O-AZB) ₂] ⁺	-0.44, -0.88	0.44	+ 1.51	1.95
[(TTP)P ^V (-O-AZN) ₂] ⁺	-0.43, -0.91, -1.13	0.48	+ 1.62	2.05

^a Error limits: $E_{1/2}$, ± 0.03 V. ^b $\Delta E_{1/2} = E_{1/2}^R(2) - E_{1/2}^R(1)$, i.e., the potential difference between the first and second one-electron reductions. ^c These potentials are for the “free” azophenols. ^d E_{CT} refers to the charge transfer state representing: azoarene⁺–P(V)porphyrin⁻.

the other hand, the effect due to the substitution of axial chlorides by the azoaryloxo ligands is minimal for the porphyrin pyrrole- β and meso-aryl proton resonances (see Figure 2 and Table 1). However, in the ³¹P NMR spectrum, signals due to the central phosphorus ions of [(TTP)P^V(-O-L)₂]⁺ (L = AZM, AZT, AZB, or AZN) were seen to be shifted downfield ($\delta = -194.9$ to -197.4 ppm, see Table 1) compared to that of [(TTP)P^VCl₂]⁺ ($\delta = -229.4$ ppm) but are within the typical range expected for hexa-coordinated diaryloxo P(V) porphyrins.^{32,33,39} Further support for the structural integrity of these new P–A systems comes from the FAB mass spectral data (see the Experimental Section). Mass spectrum of each of these hydroxide salts of P(V) porphyrins showed only a low intensity peak due to the parent [M+OH]⁺ ion, but peaks due to the fragments obtained upon elimination of the hydroxide ion and also those obtained upon successive removal of the two axial azoarene ligands were found to be intense.

Table 2 summarizes the redox potential data (CH₃CN, 0.1 M TBAP) of the P–A conjugates obtained by the differential pulse voltammetric study. Except for [(TTP)P^V(-O-AZN)₂]⁺ which showed three reduction peaks, each investigated porphyrin was found to undergo two stepwise reduction reactions. Wave-analysis (cyclic voltammetry) suggested that most of these electrode processes represent reversible ($i_{pc}/i_{pa} = 0.9$ – 1.0) and diffusion controlled ($i_{pc}/\nu^{1/2} = \text{constant}$ in the scan rate (ν) range 50–500 mV s⁻¹) one-electron transfer ($\Delta E_p = 60$ – 70 mV; $\Delta E_p = 65 \pm 3$ mV for Fc⁺/Fc couple) reactions.⁴⁰ On the other hand, the second and also the third reduction steps of [(TTP)P^V(-O-AZN)₂]⁺ are found to be either quasireversible ($E_{pa} - E_{pc} = 90$ – 200 mV and $i_{pc}/i_{pa} = 0.2$ – 0.7 in the scan rate (ν) over the range of 100–500 mV s⁻¹). Based on the redox potential data reported earlier for various P(V) porphyrins of the type [(por)P(X)₂]⁺ (where por = either a meso-tetraaryl porphyrin or the octaethyl porphyrin and X = Cl, OH, O(Si(CH₃)₃), OCH₃, or OR where R is an aryl group)^{32,41,42} and also on the basis of the diagnostic criteria developed by Fuhrhop, Kadish, and Davis for porphyrin ring reduction⁴³ ($\Delta E_{1/2}$, i.e., the difference in potential between the first one-electron and second one-electron addition = 0.42 ± 0.05 V; see Table 2 where $\Delta E_{1/2} = 0.42$ – 0.48 V), the first two reduction waves observed for the P–A conjugates investigated here can be assigned to successive, one-electron additions to the porphyrin ring. The third reduction peak observed for [(TTP)P^V(-O-AZN)₂]⁺ at -1.13 V is then a consequence of electron addition to the bound nitroaromatic axial ligands.

Scanning the potential in the positive range (0–1.8 V) for solutions containing these porphyrins gave ill-defined voltammograms with a large background current. However, all of the azophenols employed here for synthesis of the aryloxo P(V) porphyrins could be irreversibly oxidized in CH₃CN, 0.1 M TBAP. These data are summarized in Table 2.

UV–visible spectrum of a representative P–A conjugate [(TTP)P^V(-O-AZM)₂]⁺ is illustrated in Figure 3A (top

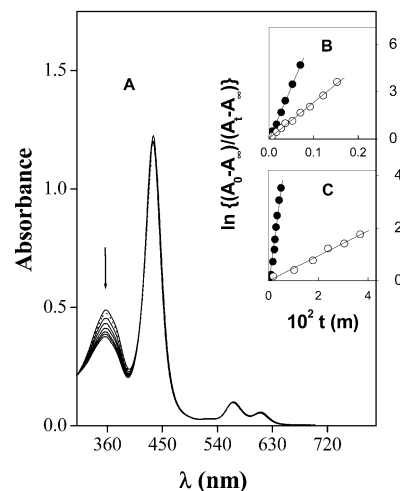


Figure 3. (A) Top curve: UV–visible spectrum of 5.9×10^{-5} M [(TTP)P^V(-O-AZM)₂]⁺ in CH₃CN. The subsequent lower traces are the spectra resulting from continuous irradiation of the solution at 345 \pm 5 nm for 1, 2, 5, 7, 9, 12, and 16 min, respectively (PTI 150 W Xe-arc lamp model A1010, PTI model 1366-MONO monochromator). The dotted curve close to the top one is the spectrum obtained after keeping the irradiated solution in the dark for several hours. (B) Comparison of the plots of $\ln\{(A_0 - A_\infty)/(A_t - A_\infty)\}$ vs t for the photochemical forward reactions of [(TTP)P^V(-O-AZM)₂]⁺ (○) and AZM(OH) (●) and (C) corresponding plots for the thermal back reactions. All the reactions were carried out at 293 ± 3 K.

TABLE 3: UV–Visible Data ^a

compound	λ_{max} , nm (log ϵ)			
	Q bands		B band	UV
[(TTP)P ^V (OH) ₂] ⁺	602 (3.94)	559 (4.19)	431 (5.41)	
[(TTP)P ^V (-O-AZM) ₂] ⁺	612 (3.90)	567 (4.13)	436 (5.21)	360 (4.77)
AZM				354 (4.25)
[(TTP)P ^V (-O-AZT) ₂] ⁺	610 (3.82)	566 (4.06)	437 (5.15)	348 (4.75)
AZT				345 (4.33)
[(TTP)P ^V (-O-AZB) ₂] ⁺	610 (4.03)	566 (4.28)	437 (5.36)	341 (4.86)
AZB				342 (4.50)
[(TTP)P ^V (-O-AZN) ₂] ⁺	610 (3.98)	565 (5.23)	440 (5.34)	360 (4.89)
AZN				367 (4.66)

^a Spectra were taken in CH₂Cl₂. Error limits: λ_{max} , ± 1 nm; log ϵ , $\pm 10\%$.

curve), and the wavelengths of maximum absorption (λ_{max}) and the molar extinction coefficient (log ϵ) values of all of the new P–A conjugates and the corresponding precursor compounds are summarized in Table 3. As seen, each new P(V) porphyrin investigated here shows what is called a “normal electronic absorption spectrum” with one intense Soret band (436–440 nm) and two less intense Q bands (565–567 and 610–612 nm) in the visible region.^{32, 42} These bands essentially originate from the π – π^* transitions involving the porphyrin macrocycle.⁴⁴ Each new P–A conjugate also shows a moderately intense band in the UV region (341–360 nm) that is absent in the spectrum of [(TTP)P^V(OH)₂]⁺ but is the major band in the spectra of the

TABLE 4: Kinetic Data on the cis ↔ trans Isomerization Reactions and Singlet and Triplet State Properties of the P–A Conjugates in CH₃CN^a

compound	ϕ_{t-c}	$k_{t-c} \text{ s}^{-1} (\times 10^{-3})$	$k_{c-t} \text{ s}^{-1} (\times 10^{-3})$	k_{t-c}/k_{c-t}	$\phi_t^i (\times 10^{-2})$	$\phi_t^c (\times 10^{-2})$	$\tau_T, \mu\text{s} (\phi_T)^b$
[(TTP)P ^v (-O-AZM) ₂] ⁺	0.022	4.74	0.031	153	0.15	0.09	35.1 (0.86)
AZM	0.12	14.04 (2.96) ^c	3.43 (110) ^c	4.1			
[(TTP)P ^v (-O-AZT) ₂] ⁺	0.017	3.64	0.025	146	0.54	0.32	20.9 (0.98)
AZT	0.09	10.23 (2.81) ^c	1.86 (75) ^c	5.5			
[(TTP)P ^v (-O-AZB) ₂] ⁺	0.013	3.15	0.022	143	1.14	0.71	32.4 (1.12)
AZB	0.20	17.12 (5.43) ^c	1.82 (83) ^c	9.4			
[(TTP)P ^v (-O-AZN) ₂] ⁺	0.016	4.37	0.024	182	3.56	2.67	29.4 (1.02)
AZN		<i>d</i>	<i>d</i>				

^a Error limits: ϕ_{t-c} and k_{t-c} , $\pm 8\%$; k_{c-t} , $\pm 5\%$; ϕ_t^i , ϕ_t^c and τ_T , $\pm 10\%$; ϕ_T , $\pm 12\%$. ^b τ_T of [(TTP)P^v(OH)₂]⁺ is 23.6 μs under the same experimental conditions of solvent and excitation wavelength. The ϕ_T values are reported in relation to that of [(TTP)P^v(OH)₂]⁺ (assumed to be unity). ^c Values given within the parentheses refer to ratios of the rates of isomerizations for the free and the complexed azoarenes (i.e., $k_{t-c}(A)/k_{t-c}(P-A)$ for the trans-to-cis case and $k_{c-t}(A)/k_{c-t}(P-A)$ for the cis-to-trans case). ^d The photochemical reaction could not be monitored in this case.

free azoarenes (see Table 3). Therefore, the origin of this band is ascribed to a transition involving the axial trans azoarene subunits of these bichromophoric systems. It should be noted that the UV–visible spectra of these P–A systems are essentially a summation of the spectra of [(TTP)P^v(OH)₂]⁺ and the corresponding free azoarene precursors (1:2 molar ratio), with the porphyrin Soret and Q bands clearly distinguishable from absorption because of the two axial azoarene moieties.

cis–trans Isomerization. The spectroscopic and electrochemical features of the new P–A conjugates described above suggest that the electronic communication between the porphyrin and the azoarene chromophores is quite negligible. More importantly, the UV–visible data suggest that it is possible to individually address photochemistry of the porphyrin and the azoarene subunits in these bichromophoric systems. Accordingly, continuous irradiation of each of these P–A conjugates (5.9×10^{-5} M, CH₃CN) at 345 ± 5 nm resulted in a time-dependent decrease of their absorption band centered at ~ 350 nm concomitant with a slight increase of absorption in the B-band region as illustrated in Figure 3A for [(TTP)P^v(-O-AZM)₂]⁺. There was no noticeable absorption change in the Q-band region of the spectrum suggesting that the porphyrin chromophore is photochemically inactive under these experimental conditions of solvent and excitation wavelength. Increase of absorption in the B-band region can thus be attributed to absorption by the cis form of the azoarene moiety.⁴⁵ The reverse thermal reaction was also spectrally monitored, and the initial spectrum in each case could be recovered quantitatively (Figure 3A). These observations clearly suggest the occurrence of reversible cis–trans isomerization of the porphyrin-bound azoarene subunits in this class of P–A conjugates.

It is of interest to know the percentage of trans-to-cis isomerization, but the presence of strongly absorbing Soret band in the region where the cis form absorbs (400–450 nm) precluded us from evaluating this parameter. In addition, the ¹H NMR spectra recorded immediately after 30 min irradiation of these P–A conjugates (samples were kept at -4 °C until the measurements were made upon attainment of the PSE state) did not show separate peaks for the cis form. However, the peaks due to various protons on the two axial azoarene subunits were found to be slightly broader for the irradiated samples compared to the corresponding protons of the starting trans compound.⁴⁶ This situation is unlike the one reported for the azobenzene interspersed bis-rhodium complexes,¹⁰ where ¹H NMR peaks of both the cis and trans forms have been clearly discernible in the PSE state. It is possible that intrinsic differences between the proton resonances of the cis and trans forms of the axially bound azoarene ligands in our P–A conjugates are offset by the strong ring current effect exerted by the basal porphyrin macrocycle.

In any case, it was possible to easily evaluate the rates of photochemical trans-to-cis (k_{t-c}) and thermal cis-to-trans (k_{c-t}) conversions of these P–A conjugates by monitoring the changes in the absorbance values at the peak maxima of azoarene chromophores. The rates were found to follow first-order kinetics. Representative plots of $\ln\{(A_0 - A_\infty)/(A_t - A_\infty)\}$ vs t are illustrated in Figure 3 (insets B and C) and the values of k_{t-c} , Φ_{t-c} , and k_{c-t} thus obtained are summarized in Table 4. Several interesting observations can be made from an analysis of the data given in this Table.

(i) Both k_{t-c} and Φ_{t-c} values for the porphyrin-bound azoarene ligands are an order of magnitude lower than the corresponding values for the precursor free azophenols. A comparison of the plots shown in Figure 3B for AZM(OH) and [(TTP)P^v(-O-AZM)₂]⁺ is illustrative in this regard. It should be noted here that the slower rates and the lower quantum yields observed for the trans-to-cis isomerization of the P–A conjugates are not due to the competitive absorption due to the porphyrin chromophore because absorption due to the porphyrin part of these conjugates does not exceed ca. 10% at 345 nm. In addition, rates of the thermal cis-to-trans isomerization reactions of the P–A conjugates are also lower than those of the corresponding free azoarene precursors (see Figure 3C). We thus rationalize that slower rates and lower quantum yields of the isomerization reactions observed here for the P–A conjugates are due to the enlargement of the rotor volume for the motion of isomerization that is a consequence of binding of these azoarenes to large porphyrin molecule.⁴⁷ A similar interpretation has been made for the azoarene interspersed bisterpyridine complexes of rhodium(III) mentioned above, for which the rates of isomerization were found to be slower than the corresponding “uncomplexed” azoarenes.¹⁰

(ii) As such, the value of k_{c-t} is lower than the k_{t-c} for each azoarene irrespective of whether it is bound at the phosphorus-(V) center or is in its free form. This observation is consistent with the fact that the thermal reverse isomerizations are invariably slow compared to the photochemical trans-to-cis conversions for various azoarene compounds.⁴⁵ On the other hand, photochemical cis-to-trans isomerizations are known to be fast,⁴⁵ but prolonged irradiation of the cis forms of these P–A conjugates in the 400–430 nm region did not result in the expected conversion because of the competing absorption by the strongly absorbing porphyrin chromophore.

(iii) Although the value of k_{c-t} is lower than k_{t-c} for each azoarene irrespective of whether it is bound at the phosphorus-(V) center or not, it is observed that the ratios k_{t-c}/k_{c-t} for the bound forms are higher (143–182) than the corresponding values for the free forms (4.1–9.4), Table 4. A more detailed analysis reveals that ratios of the rates of cis-to-trans isomerizations for the free (A) and complexed (P–A) azoarenes (i.e.,

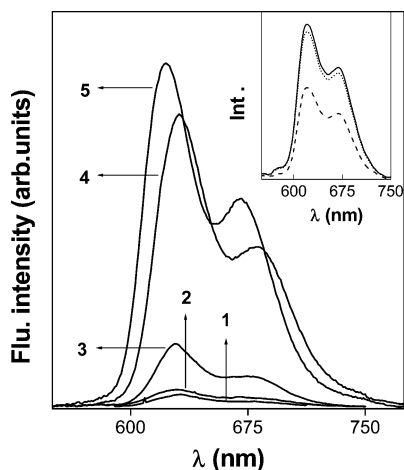


Figure 4. Comparison of the fluorescence spectra of equiabsorbing solutions (O. D. = 0.12, CH₃CN, $\lambda_{\text{exc}} = 565$ nm) of the “trans forms” of [(TTP)P^V(-O-AZM)₂]⁺ (1), [(TTP)P^V(-O-AZT)₂]⁺ (2), [(TTP)P^V(-O-AZB)₂]⁺ (3), and [(TTP)P^V(-O-AZN)₂]⁺ (4) with that of [(TTP)P^V(OH)₂]⁺ (5) Inset: Fluorescence spectra of “cis and trans forms” of 5.9×10^{-5} M [(TTP)P^V(-O-AZT)₂]⁺ in CH₃CN: (—) unirradiated “trans form”, (- - -), “cis form” obtained upon irradiating the above solution for 30 min at 345 ± 5 nm and (...) “trans form” recovered from the back thermal reaction of the “cis form” of the complex. $\lambda_{\text{exc}} = 565$ nm in each case.

$k_{\text{c} \rightarrow \text{t}}(\text{A})/k_{\text{c} \rightarrow \text{t}}(\text{P-A})$ are higher (75–110) than the corresponding ratios for the trans-to-cis isomerizations (i.e., $k_{\text{t} \rightarrow \text{c}}(\text{A})/k_{\text{t} \rightarrow \text{c}}(\text{P-A})$), which are < 6), Table 4. This fact can also be understood by comparing slopes of the kinetic curves in Figure 3, parts B ($k_{\text{t} \rightarrow \text{c}}(\text{A})/k_{\text{t} \rightarrow \text{c}}(\text{P-A})$) and C ($k_{\text{c} \rightarrow \text{t}}(\text{A})/k_{\text{c} \rightarrow \text{t}}(\text{P-A})$). Clearly, linking the azoarene to the porphyrin seems to affect the thermal back reaction more than it does affect the photochemical forward reaction. The reason for this variation is unclear at the present, but it should be noted that activation mechanisms for the cis-to-trans (thermal) and trans-to-cis (photochemical) reactions are different.

(iv) There seems to be no apparent relationship between the rates of photochemical/thermal isomerization reactions and the electron donating/withdrawing nature of the substituent located at the para position of the axial azoarene moieties of the P–A conjugates.⁴⁸

Thus, the kinetic data presented above clearly suggest that the cis ↔ trans isomerization reactions of the P–A conjugates investigated here occur smoothly and reversibly. With this information in hand, we set out to explore the photoswitching function of these conjugates, the results of which are described in the next section.

Photoswitching Function. Excitation of each P–A conjugate at 345 nm resulted in no fluorescence emanating from the trans form of the two axial azo chromophores in CH₃CN solutions, as is the case with the precursor free *trans*-azoarenes. On the other hand, the porphyrin component of each complex showed a fluorescence spectrum ($\lambda_{\text{exc}} = 465/565$ nm) that is typical of a hexa-coordinated P(V) porphyrin with the singlet state energy (E_{0-0}) being close to (2.04 ± 0.1 eV) that of [(TTP)P^V(OH)₂]⁺.^{32,44} Although fluorescence quantum yields of the trans forms ($\phi_{\text{f}}^{\text{t}}$) of [(TTP)P^V(-O-AZM)₂]⁺, [(TTP)P^V(-O-AZT)₂]⁺, and [(TTP)P^V(-O-AZB)₂]⁺ are found to be less than that of the reference compound [(TTP)P^V(OH)₂]⁺ ($\Phi_{\text{f}} = 0.045$), ($\phi_{\text{f}}^{\text{t}}$) of [(TTP)P^V(-O-AZN)₂]⁺ is close to that of [(TTP)P^V(OH)₂]⁺ within the experimental error (see, Figure 4 and Table 4). Interestingly, fluorescence intensities due to the cis forms ($\phi_{\text{f}}^{\text{c}}$) of these four P–A conjugates also followed a similar trend but are all lower than the values of the corresponding trans forms.⁴⁹

TABLE 5: Fluorescence Data in Various Solvents^a

compound	λ_{em} , nm %Q			
	toluene	CH ₂ Cl ₂	CH ₃ CN	DMF
[(TTP)P ^V (OH) ₂] ⁺	619, 669	622, 674	622, 671	623, 672
[(TTP)P ^V (-O-AZM) ₂] ⁺	631, 680	630, 681	631, 679	629, 677
	94	94	97	98
[(TTP)P ^V (-O-AZT) ₂] ⁺	634, 681	631, 680	631, 680	628, 675
	91	94	88	93
[(TTP)P ^V (-O-AZB) ₂] ⁺	631, 675	630, 682	630, 680	633, 674
	79	73	75	80
[(TTP)P ^V (-O-AZN) ₂] ⁺	634, 679	630, 679	630, 682	633, 679
	26	–13	21	29

^a Error limits: λ_{em} , ±2 nm; Q, ±10%.

Thermal back reaction regenerated the fluorescence intensity of the trans form in each case and this fact is illustrated in Figure 4 (inset) for [(TTP)P^V(-O-AZT)₂]⁺. This photochemical/thermal trans ↔ cis interconversion was repeated 8–10 times with less than 5% loss of the material (UV–visible and fluorescence) establishing that the P–A conjugates investigated here are effective and stable photoswitches.

What is the origin of weak fluorescence observed for these P–A conjugates and what is the mechanism of their photo-switching function? A variety of excited-state processes including excitation energy transfer (EET), photochemical dissociation of the azoarene ligands, enhanced internal conversion and intersystem crossing, ion-association, photoinduced electron transfer (PET), etc. can be thought of to be operative in the quenching of fluorescence observed for these azoarene appended P(V) porphyrins. Obviously, it is not going to be easy to estimate the contribution from each of these excited-state processes. However, the following observations can be made in this regard.

(i) The singlet state energy of the “porphyrin part” of each P–A conjugate (2.04 ± 0.1 eV) lies lower than that of the aromatic axial ligands (ca. >3.0 V). Moreover, excitation spectra of none of these P–A conjugates (emission collected at 600/650 nm, porphyrin fluorescence bands) showed absorption corresponding to the azoarene chromophore. Thus, fluorescence quenching observed here for these P–A conjugates is not due to energy transfer between the azoarene and porphyrin subunits.

(ii) Neither was the fluorescence of [P(TTP)(OH)₂]⁺ found to be quenched upon addition of free azoarenes AZM(OH), AZT(OH), AZB(OH), and AZN(OH) nor was there any rate enhancement for the thermal back reactions of the P–A conjugates in the presence of externally added free azoarenes (upto ca. 6 equivalents, mol/mol). These observations indicate that there is no photochemical dissociation of azoarene ligands from our P–A conjugates, under the experimental conditions employed during this study.

(iii) The triplet quantum yields and also the corresponding lifetimes of these P–A conjugates are found to be not only quite similar to each other but also close to those of [P(TTP)(OH)₂]⁺ (see Table 4). Thus, the diminution in the fluorescence quantum yields of the P–A conjugates is not a consequence of enhanced intersystem crossing.

(iv) Fluorescence spectra of the “trans forms” of the P–A conjugates have been measured in four different solvents, and the emission maxima as well as the %Q values (equn. 2) are given in Table 5.

$$\%Q = \{[\phi_{\text{f}}^{\text{t}}]_{\text{[P(TTP)(OH)}_2]^+} - \phi_{\text{f}}^{\text{t}}]_{\text{P-A}} / \phi_{\text{f}}^{\text{t}}]_{\text{[P(TTP)(OH)}_2]^+}\} \times 100 \quad (2)$$

An inspection of the data summarized in Table 5 reveals that the general dependence of %Q values on the electron donating/

withdrawing ability of the axial ligand and also on the solvent polarity cannot be rationalized solely on the basis of differences in the rates of internal conversion and intersystem crossing reactions of the azoarene appended porphyrins among themselves and also in relation to the dichloro/dihydroxy analogue. Therefore, contribution of these nonradiative processes to the overall decrease in the quantum yield values is considered to be the minimum for the P–A conjugates investigated here. Ion association is another phenomenon that is imminent in these positively charged P–A conjugates, and the extent of this process is expected to be dependent on the solvent properties and also on the structure of the fluorophore. Currently, there exists no direct or indirect evidence/s to show the correspondence between the trends observed for the ϕ_f^1 values and the extent of ion association in these complexes, as is the case with the previously reported positively charged aryloxo P(V) porphyrins.³²

On the other hand, an intramolecular PET from the axial azobenzene donors to the singlet excited state of the basal phosphorus(V) porphyrin seems to be the most probable pathway for the quenching of fluorescence in these axial-bonding type complexes. As described below, this interpretation is consistent with (i) exoergicity for such a PET reaction, (ii) variation of the fluorescence intensity with the solvent polarity, and (iii) a similar interpretation made earlier for analogous axial bonding type P(V) porphyrins.³²

The free energy changes for the photoinduced electron-transfer reactions (ΔG_{PET}) from the axial azoarenes to the singlet states of the basal porphyrin subunits are calculated using eq 3

$$\Delta G_{\text{PET}} = E_{\text{CT}} - E_{0-0} \quad (3)$$

where E_{CT} refers to the charge transfer state representing the azoarene⁺–P(V)porphyrin^{•–} and E_{0-0} is energy of the singlet state of the porphyrin. The E_{CT} (Table 2) and E_{0-0} (2.04 ± 0.1 eV) values are evaluated from the electrochemical and absorption/fluorescence spectral data of these P–A conjugates, respectively. The ΔG_{PET} values thus calculated are negative for [(TTP)P^V(-O-AZM)₂]⁺ (–0.38 eV), [(TTP)P^V(-O-AZT)₂]⁺ (–0.12 eV), and [(TTP)P^V(-O-AZB)₂]⁺ (–0.09 eV), the cases in which the fluorescence quenching has been observed.⁵⁰ A similar PET based mechanism has been proposed earlier for the fluorescence quenching (in relation to [(TTP)P^V(OH)₂]⁺) observed for a series of bis(aryloxo) phosphorus(V) porphyrins reported by us³² and for the “wheel-and-axle” type phosphorus(V) porphyrins reported by Shimidzu and co-workers.⁵¹ In addition, consistent with this analysis is the fact that ΔG_{PET} is positive (+0.01 eV) for [(TTP)P^V(-O-AZN)₂]⁺ which is endowed with the electron withdrawing nitro group at the axial azobenzene ligands and whose ϕ_f^1 is close to that of [(TTP)P^V(OH)₂]⁺. Finally, the observed general decrease of the ϕ_f^1 values (or the increase in the %Q values, see Table 5) with the exothermicity of the reaction and also with increasing polarity of the solvent are both consistent with the participation of a charge transfer state in the excited-state deactivation for these compounds.⁵²

Thus, accepting that a PET is occurring between the axial ligand and the singlet porphyrin in these donor–acceptor complexes, the photoswitching function demonstrated here can be rationalized in terms of the distance dependence of PET which is well documented in the literature.⁵³ As schematically represented in Figure 5, the distance between the basal porphyrin and the axial ligand in the “cis form” is shorter than that in the “trans form” explaining the additional fluorescence quenching observed for the former isomer.⁵⁴

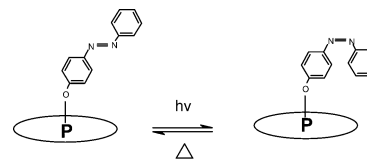


Figure 5. Photoswitching function induced by the reversible cis–trans isomerization of the axial azoarene chromophores in the P–A conjugates investigated in this study.

It is pertinent to compare here the photoswitching abilities of the previously reported porphyrin–azobenzene systems with that of the P–A conjugates investigated in the present study. Studies on the covalently connected azobenzene–porphyrin conjugates reported by Hunter and Sarson revealed that photochemistry of the porphyrin components of these novel chromophoric assemblies is essentially unaltered, but the photochemical isomerization of their azobenzene components could not be detected.¹⁴ Similarly, electro-switch and proton-switch properties of an supramolecular ensemble comprising of [(TPP)Zn^{II}] and axially ligated 4-(phenylazo)pyridine have been reported, but the effect of cis–trans isomerization on the luminescence properties of this system was not observed.¹⁵ On the other hand, fluorescence properties of the early azobenzene–porphyrin systems reported by several groups were not investigated in detail.^{16–18} Although While this work was in progress, photoswitching features of an azobenzene-linked diporphyrin complex have been described.¹³ However, because of the extensive absorption by the two dissimilar porphyrin chromophores in the UV–visible region, spectral detection of the cis–trans isomerization in this system was not as facile as demonstrated here for our P–A compounds.

In conclusion, the P–A conjugates reported here fulfill the key criteria that are desirable in an azobenzene-based, red-sensitive photochromic material: (i) These compounds are easily synthesizable and stable molecular species, (ii) they exhibit distinct absorption spectral properties such that the photochemical/photophysical properties of the azoarene and porphyrin chromophores can be individually addressed, (iii) the photochemical trans-to-cis and thermal cis-to-trans isomerization reactions of their axial azoarene chromophores are facile and reversible processes, and (iv) their photoswitching function, which is stable over many photochemical/thermal cycles, can be easily sensed by the luminescence method illustrating the utility of this class of molecules in potential applications.

Acknowledgment. Financial assistance received for this work from the CSIR (New Delhi) and BRNS (Mumbai, India) is gratefully acknowledged. We thank NCUFP (Chennai, India) and Dr. P. Ramamurthy for the triplet state data.

References and Notes

- (1) *Molecular Switches*; Feringa, B. L., Ed.; Wiley-VCH Verlag GmbH: Weinheim: Germany, 2001.
- (2) Special issue on Photochromism: Memories and Switches. *Chem. Rev.* **2000**, 1683.
- (3) Balzani, V.; Credi, A.; Raymo, F. M.; Stoddart, J. F. *Angew. Chem., Int. Ed.* **2000**, 39, 3348.
- (4) Belser, P.; Bernhard, S.; Blum, C.; Beyeler, A.; de Cola, L.; Balzani, V. *Coord. Chem. Rev.* **1999**, 190, 155.
- (5) de Silva, A. P.; Gunaratne, H. Q. N.; Gunnlaugsson, T.; Huxley, A. J. M.; McCoy, C. P.; Rademacher, J. T.; Rice, T. E. *Chem. Soc. Rev.* **1997**, 26, 1515.
- (6) Yam, V. W.-W.; Lau, V. C.-Y.; Wu, L.-X. *J. Chem. Soc., Dalton Trans.* **1998**, 1461.
- (7) Archit, A.; Vogtle, F.; de Cola, L.; Azzellini, G. C.; Balzani, V.; Ramanujan, P. S.; Berg, R. H. *Chem. Eur. J.* **1998**, 4, 699.
- (8) Kurosawa, M.; Nankawa, T.; Matsuda, T.; Kubo, K.; Kurihara, M.; Nishihara, H. *Inorg. Chem.* **1999**, 38, 5113.

- (9) Kurihara, M.; Matsuda, T.; Hirooka, A.; Yukata, T.; Nishihara, H. *J. Am. Chem. Soc.* **2000**, *122*, 12373.
- (10) Yukata, T.; Kurihara, M.; Kubo, K.; Nishihara, H. *Inorg. Chem.* **2000**, *39*, 3438.
- (11) Kume, S.; Kurihara, M.; Nishihara, H. *Chem. Commun. (Cambridge)* **2001**, 1656.
- (12) Yukata, T.; Mori, I.; Kurihara, M.; Mizutani, J.; Kubo, K.; Furusho, S.; Matsumura, K.; Tamai, N.; Nishihara, H. *Inorg. Chem.* **2001**, *40*, 4986 and references therein.
- (13) Tsuchiya, S. *J. Am. Chem. Soc.* **1999**, *121*, 48.
- (14) Hunter, C. A.; Sarson, L. D. *Tetrahedron Lett.* **1996**, *37*, 699.
- (15) Otsuki, J.; Harada, K.; Araki, K. *Chem. Lett.* **1999**, 269.
- (16) Autret, M.; le Plouzennec, M.; Moinet, C.; Simmonneaux, G. *Chem. Commun.* **1994**, 1169.
- (17) Hombrecher, H. K.; Ludtke, K. *Tetrahedron* **1993**, *49*, 9489.
- (18) Neumann, K. H.; Vogtle, F. *Chem. Commun. (Cambridge)* **1988**, 520.
- (19) Reddy, D. R.; Maiya, B. G. *Chem. Commun. (Cambridge)* **2001**, 117.
- (20) Perrin, D. D.; Armarego, W. L. F.; Perrin, D. R. *Purification of laboratory Chemicals*; Pergamon: Oxford, 1986.
- (21) Fuhrhop, J.–H.; Smith, K. M. In *Porphyrins and Metalloporphyrins*; Smith, K. M., Ed.; Elsevier: Amsterdam, 1975; p 769.
- (22) Barbour, T.; Belcher, W. J.; Brothers, P. J.; Rickard, C. E. F.; Ware, D. C. *Inorg. Chem.* **1992**, *31*, 746.
- (23) *Vogel's Text Book of Practical Organic Chemistry* (Revised by Furniss, B. S.; Hannaford, A. J.; Smith, P. W. G.; Tatchell, A. R.), 5th ed.; Longman (ELBS): Essex, U.K., 1991.
- (24) Ambrose, A.; Maiya, B. G. *Inorg. Chem.* **2000**, *39*, 4256.
- (25) Ambrose, A.; Maiya, B. G. *Inorg. Chem.* **2000**, *39*, 4264.
- (26) Hariprasad, G.; Dahal, S.; Maiya, B. G. *J. Chem. Soc., Dalton Trans.* **1996**, 3429.
- (27) Harriman, A.; Davila, J. *Tetrahedron* **1989**, *45*, 4737.
- (28) Lackowicz, J. R. *Principles of Fluorescence Spectroscopy*; Plenum: New York, 1983.
- (29) Jayanthi, S. S.; Ramamurthy, P. *Phys. Chem. Chem. Phys.* **1999**, *1*, 4751.
- (30) Bortolus, P.; Monti, S. *J. Phys. Chem.* **1979**, *83*, 648.
- (31) Hatchard, C. G.; Parker, C. A. *Proc. R. Soc. London* **1956**, *A235*, 518.
- (32) Rao, T. A.; Maiya, B. G. *Inorg. Chem.* **1996**, *35*, 4829.
- (33) Rao, T. A.; Maiya, B. G. *Chem. Commun.* **1995**, 939.
- (34) Giribabu, L.; Rao, T. A.; Maiya, B. G. *Inorg. Chem.* **1999**, *38*, 4971.
- (35) Kumar, A. A.; Giribabu, L.; Reddy, D. R.; Maiya, B. G. *Inorg. Chem.* **2001**, *40*, 6757.
- (36) Giribabu, L.; Kumar, A. A.; Neeraja, V.; Maiya, B. G. *Angew. Chem., Int. Ed.* **2001**, *40*, 3621.
- (37) Susumu, K.; Segawa, H.; Shimidzu, T. *Chem. Lett.* **1995**, 929.
- (38) Abraham, R. J.; Bedford, G. R.; McNeillie, D.; Wright, B. *Org. Magn. Reson.* **1980**, *14*, 418.
- (39) *Multinuclear NMR*; Mason, J., Ed.; Plenum Press: New York, 1987; p 369.
- (40) Nicholson, R. S.; Shain, I. *Anal. Chem.* **1964**, *36*, 706.
- (41) Marrese, C. A.; Carrano, C. J. *Inorg. Chem.* **1984**, *23*, 3961.
- (42) Liu, Y. H.; Benassy, M.-F.; Chojnacki, S.; D'Souza, F.; Barbour, T.; Blecher, J. W.; Brothers, P. J.; Kadish, K. M. *Inorg. Chem.* **1994**, *33*, 4480.
- (43) Fuhrhop, J. H.; Kadish, K. M.; Davis, D. G. *J. Am. Chem. Soc.* **1973**, *95*, 5140.
- (44) Sayer, P.; Gouterman, M.; Connell, C. R. *Acc. Chem. Res.* **1982**, *15*, 73.
- (45) Rau, H. In *Photochromism: Molecules and Systems*; Durr, H. B., Laurent, H., Eds.; Elsevier: Amsterdam, 1990; pp 165–192.
- (46) Broadening of peaks was found to be more for the resonances due to protons on the “remote” aryl ring than it is for those present on the ring directly attached to the P(V) ion.
- (47) This analysis intrinsically assumes that the isomerization proceeds via a rotational (around the N=N bond) mechanism for which contributions from the substituent-induced dipolar structures are known to lower the barrier (see, for example, Wildes, P. D.; Pacifici, J. G.; Irick, G., Jr.; Whitten, D. G. *J. Phys. Chem.* **1971**, *93*, 2004). Within the limited set of data available in hand, plots of k_{t-c} (ϕ_{t-c}) or k_{c-t} of the P–A conjugates vs Hammett coefficients of their para substituents were constructed and were found to be not strictly linear. On the other hand, low activation barriers are known to be generally compatible with an inversion mechanism (see ref: Sueyoshi, T.; Nishimura, N.; Yamamoto, S.; Hasegawa, S. *Chem. Lett.* **1974**, 1131). The activation energies measured for the thermal back reactions for [(TTP)P^v(-O-AZM)₂]⁺, [(TTP)P^v(-O-AZT)₂]⁺, [(TTP)P^v(-O-AZB)₂]⁺, and [(TTP)P^v(-O-AZN)₂]⁺ are 15.20, 10.57, 12.91, and 13.92 kcal mol⁻¹ (±12%), respectively, but are found to be all higher than the activation barriers for the corresponding free azophenols (6–7 kcal mol⁻¹). Clearly, more studies involving various para-substituted azoarenes are needed to ascertain the exact mechanism of isomerization of these P–A conjugates.
- (48) On the other hand, substituents present at the 2 (2') and 6 (6') positions of azoarenes can, in principle, cause steric crowding around the interconverting azo group and hence are known to affect the isomerization rates (see, for example, Gegiou, D.; Muszkat, K. A.; Fischer, E. *J. Am. Chem. Soc.* **1968**, *90*, 3907).
- (49) Fluorescence spectra were measured immediately upon attainment of the PSE state.
- (50) It should be noted here that the ΔG_{PET} values vary in an order that is consistent with the electron donating ability of the 4'-substituent on the axial azoarene subunit.
- (51) Susumu, K.; Kunimoto, K.; Segawa, H.; Shimidzu, T. *J. Phys. Chem.* **1995**, *99*, 29.
- (52) Suppan, P. *Chimica* **1988**, *42*, 320.
- (53) Wasielewski, M. R. In *Photoinduced Electron Transfer*; Fox, M. A., Chanon, M., Eds.; Elsevier: Amsterdam, 1988; Part A, pp 123–160.
- (54) The values of ϕ_f^c/ϕ_f^t are quite similar for [(TTP)P^v(-O-AZM)₂]⁺, [(TTP)P^v(-O-AZT)₂]⁺, and [(TTP)P^v(-O-AZB)₂]⁺ (0.60 ± 0.2; i.e., nearly 40% quenching in each case) suggesting that the change in the D–A distance while going from the trans to the cis form is quite similar for each of these conjugates.